IET Science, Measurement & Technology

Research Article

IET Journals
The Institution of Engineering and Technology

Evaluations of the apparent soil resistivity and the reflection factor effects on the grounding grid performance in three-layer soils

ISSN 1751-8822
Received on 21st June 2018
Revised 24th October 2018
Accepted on 21st January 2019
doi: 10.1049/iet-smt.2018.5336
www.ietdl.org

Osama E. Gouda[1] ✉, Tamer El-Saied[2], Waleed A.A. Salem[2], Asmaa M.A. Khater[2]

[1]*Faculty of Engineering, Cairo University, Cairo, Egypt*

[2]*Faculty of Engineering, Banha University, Banha, Egypt*

✉ *E-mail: prof_ossama11@yahoo.com*

Abstract: In this study, the apparent soil resistivity evaluation is estimated for three-layer soils by four strategies and the obtained values are compared with experimental measurements done by using the four-electrode method. Different methods are suggested with the aid of IEEE 80 to estimate the apparent soil resistivity of three-layer soils, in which a grounding system consisting of a grid with rods is constructed. The effect of the reflection factor on the mesh and the step voltages, the grounding system resistance and the mesh voltage is investigated. It is concluded that the first three methods are close together, and also with the experimental findings done by the authors and others the fourth method gives some tolerance with the first three, but it is in agreement with the experimental measurements. It is concluded also that the reflection factors of non-uniform soil have significant effects on the apparent soil resistivity, the step and the mesh voltages and the ground resistance. For the verification of the calculated results, experimental model is used. It is noted that the measured values are slightly high compared with the calculated values; the reason may be due to the boundary effects of the used model.

1 Introduction

Calculation of the grounding system total resistance is one of the first steps in determining the size and basic layout of a grounding system. The soil at the most sites is non-uniform. At first glance, this may appear difficult to obtain the estimated values of grounding resistance, step voltage and mesh voltage. The grounding system resistance depends primarily on the area to be occupied by the grounding system, which is usually known in the early design stage.

Calculation of the grounding grid resistance is reported by [1–3]. Optimum design of the grounding system in a uniform and non-uniform soils using artificial neural network is presented in [4]. Simplified analysis of electrical gradients above a ground grid is investigated in [5]. Analytical expressions for the resistance of grounding systems are investigated by [6–10]. Optimum design of the substation grounding in a two-layer Earth structure is reported by Dawalibi and Mukhedkar [11], He *et al.* [12] and Sun *et al.* [13].

Different mathematical expressions and methods to compute the grounding resistance are suggested by many investigators, several computer programs based on some of these methods have been developed by Thabet [14], Phithakwong *et al.* [15], Gouda and El Dein [16], Gouda *et al.* [17] and others [18–21]. According to IEEE 80 standard [3], the grounding grid resistance must be low enough to assure that faults currents dissipate through the grounding grid into the earth, while the ground potential rise on the earth's surface must be kept under certain tolerances, i.e. step, touch and mesh voltages have to be in the safety level defined by the standard [3].

To design the most economical and efficient grounding systems, it is necessary to obtain an accurate value of the resistivity on the site. This paper includes different methods to compute the apparent resistivity of three multilayer soil structures and comparing the calculated values with the actual field measurements done by Charlton [21]. Also, the factors affecting the apparent soil resistivity of multilayer soils are investigated. Such factors for the evaluation of the grounding system in multilayer soils are:

i. The number of layers of soil structure (double and three layers are considered) and their arrangement.
ii. The thickness of each layer.
iii. The reflection factor between each layer.

The soil composition can be clay, gravel, loam, rock, sand, shale, silt, stones etc. In many locations, soil can be quite homogeneous, while other locations may be mixtures of these soil types in varying proportions. Very often, the soil composition is in layers [19]. Takahashi and Kawase [22] suggested a formula to analyse the changes of the calculated apparent resistivity of multilayer soils by using a comparison of soil resistivity-space between electrodes curves. Optimum estimation of electrical grounding parameters for a two-layered soil is obtained by Del Alamo [23]. Combined electrostatic images method to evaluate *N*-layer apparent soil resistivity and interpret sounding measurements by Wenner method is carried out by Lagacé *et al.* [24]. Slaoui *et al.* [25] proposed a method to estimate *N*-layer soil parameters for the most economical grounding system. Slaoui *et al.* [26] suggested a new method to calculate the apparent soil resistivity of multilayered soils to determine the electrical grounding parameters of *N*-layered soil. A method to estimate soil parameters of multilayered horizontal soil is estimated by Lagace and Vuong [27] and Salama *et al.* [28].

Since the methods deal with the multilayer soils grounding system are rare and complex; in this paper, models have been suggested to calculate the apparent soil resistivity of three multilayer soils, any number of layers can be shortened into two layers, then it can be reduced to one equivalent layer.

In this paper, the apparent soil resistivity evaluation in the field is estimated for multilayer soils by four methods and the obtained values are compared with experimental measurements done by using the four-electrode method and field measurements done by Charlton [21]. In this paper also different methods are suggested with the aid of IEEE 80 to estimate the apparent soil resistivity of multilayer soils containing grounding system consisting of a grid with rods. The effects of reflection factor on the mesh and step voltages and grounding system resistance and mesh voltage are investigated in this paper.

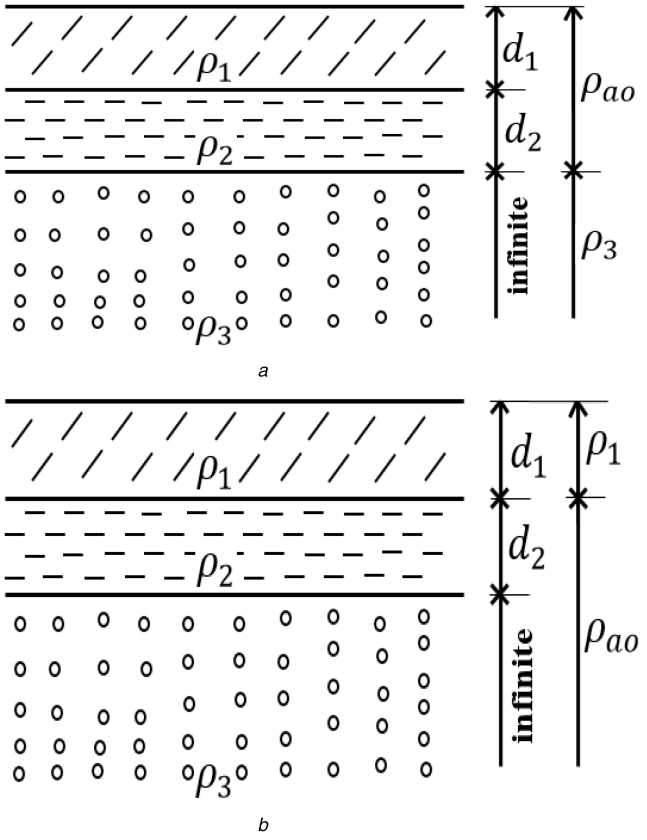

Fig. 1 *Three layers soil model*
(a) Three-layer soil, first and second layers are evaluated as ρ_{ao}, ***(b)*** Three layers soil, second and third layers are evaluated as ρ_{ao}

2 Apparent soil resistivity evaluation in the field

The apparent soil resistivity of two layers of soil can be evaluated using the following formulas that are developed by Sunde [18]:

$$\rho_{a0} = 2\left(\rho_2 - (\rho_2 - \rho_1)\cdot e^{-js}\right) - \left(\rho_2 - (\rho_2 - \rho_1)\cdot e^{-2js}\right) \quad (1)$$

where ρ_{ao} is the apparent soil resistivity between first and second layers; ρ_1 is the first layer soil resistivity; ρ_2 is the second layer soil resistivity; S is the spacing between probe electrodes of measuring soil resistivity; d_1 is the first layer of soil thickness; δ is the scaling factor; and

$$j = \delta / 2(d_1), \quad \delta = \frac{\ln(\rho_1/\rho_2) - \ln(0.0176)}{3.5}$$

The apparent soil resistivity of three layers soil can be evaluated using one of the following four methods.

2.1 First method for apparent soil resistivity evaluation

The apparent soil resistivity of three soil layers is obtained by evaluating initial apparent soil resistivity between the first and second layers represented by (ρ_{ao}) as indicated in Fig. 1*a* using the Sunde equation (1) [18]. Then, considering the initial apparent soil resistivity which evaluated between first and second layers (ρ_{ao}) as a first layer, and then considering the third layer resistivity as a second one. Thus, the apparent soil resistivity of the three layers can be obtained as follows:

$$\rho_a = 2(\rho_3 - (\rho_3 - \rho_{ao})\cdot e^{-qs}) - (\rho_3 - (\rho_3 - \rho_{ao})\cdot e^{-2qs}) \quad (2)$$

where ρ_{ao} is the apparent soil resistivity between first and second layers; ρ_a is the apparent soil resistivity of the three layers, ρ_3 is the third layer soil resistivity, d_2 is the second layer soil thickness; d_1 is the first layer soil thickness; and

$$q = \lambda / 2(d_1 + d_2), \quad \lambda = \frac{\ln(\rho_{ao}/\rho_3) - \ln(0.0176)}{3.5}$$

Calculated values versus electrode spacing of this method are shown in Fig. 2*a* using the same parameters as actual measurements that are reported by Charlton [21]. These parameters are: the first layer resistivity ρ_1 is 59 Ω m and its thickness $d_1 = 1.1$ m, the second layer of resistivity ρ_2 is 104 Ω m and has a thickness of $d_2 = 4.6$ m and the third layer of resistivity is $\rho_3 = 35$ Ω m with infinite thickness.

2.2 Second method for apparent soil resistivity evaluation

In this method, the apparent soil resistivity between second and third layers is represented by ρ_{ao} as indicated in Fig. 1*b* and it is calculated by using the equation below:

$$\rho_{a0} = 2\left(\rho_3 - (\rho_3 - \rho_2)\cdot e^{-js}\right) - \left(\rho_3 - (\rho_3 - \rho_2)\cdot e^{-2js}\right) \quad (3)$$

where ρ_3 is the third layer soil resistivity; ρ_2 is the second layer soil resistivity; d_1 is the first layer soil thickness; and j is defined as

$$j = \delta / 2(d_1), \quad \delta = \frac{\ln(\rho_2/\rho_3) - \ln(0.0176)}{3.5}$$

Then, the resultant apparent soil resistivity of the three layers will be as follows:

$$\rho_a = 2(\rho_{ao} - (\rho_{ao} - \rho_1)\cdot e^{-qs}) - (\rho_{ao} - (\rho_{ao} - \rho_1)\cdot e^{-2qs}) \quad (4)$$

where ρ_{ao} is the apparent soil resistivity between second and third layers; ρ_1 is the first layer soil resistivity; and d_1 is the first layer soil thickness

$$q = \lambda/2(d_1), \quad \lambda = \frac{\ln(\rho_1/\rho_{a0}) - \ln(0.0176)}{3.5}$$

The calculated values versus electrode spacing using this method are given in Fig. 2*a*. The data used are as that reported by Charlton [21].

2.3 Third method for apparent soil resistivity evaluation

In this method, according to the modifications done by Seedher and Arora [29] to obtain the best estimation of two-layer parameters by using Wenner four pole test data, the apparent soil resistivity of the three layers is evaluated by obtaining the initial apparent soil resistivity between first and second layers that are represented by (ρ_{ao}), and then considering the initial apparent soil resistivity of first and second layers (ρ_{ao}) as a first layer and third layer (ρ_3) as a second layer. Thus, the apparent soil resistivity of three layers will be as follows.

When $(\rho_3) > (\rho_{ao})$

$$\rho_a = \rho_{a0} + 4\rho_{a0}K_{a0}\cdot s\cdot\left[\frac{1}{\sqrt{s^2 + 4(d_1 + d_2)^2}} - \frac{1}{\sqrt{4s^2 + 4(d_1 + d_2)^2}}\right] + 4\pi V_b\cdot s\cdot\left[\sqrt{\frac{c}{c + (s/(d_1 + d_2))^\beta}} - \sqrt{\frac{c}{c + (2s/(d_1 + d_2))^\beta}}\right] \quad (5)$$

where ρ_1 is the first layer soil resistivity, ρ_2 is the second layer soil resistivity; ρ_3 is the third layer soil resistivity; d_1 is the first layer soil thickness; and d_2 is the second layer soil thickness

$$K_{a0} = \frac{(\rho_2 - \rho_1)}{(\rho_2 + \rho_1)}, \quad K_{a03} = \frac{(\rho_3 - \rho_{a0})}{(\rho_3 + \rho_{a0})}$$

$$V_b = \frac{\rho_{a0}(-K_{a0} - \ln(1 - K_{a03}))}{2\pi(d_2 + d_1)}$$

$$c = x_1 \cdot \left[\ln\left(\frac{\rho_3}{\rho_{a0}}\right)\right] \cdot x_3, \quad \beta = 2 - x_2 \cdot \left[\ln\left(\frac{\rho_3}{\rho_{a0}}\right)\right]$$

$$x_1 = 16.4133, \quad x_2 = 0.136074, \quad x_3 = 0.393468$$

However, when $(\rho_3) < (\rho_{ao})$ the finite expression for apparent resistivity is obtained as follows:

$$\rho_a = \rho_3 + \left((\rho_{a0} - \rho_3) \cdot (2e^{-u_s s} - e^{-u_2 \cdot 2s})\right) \tag{6}$$

where

$$u = u_m - \frac{(u_m - x_1) \cdot e^{-x_2}(s/(d_1 + d_2))}{d_1 + d_2}$$

$$u_m = x_3 x_4 \left(\frac{\rho_3}{\rho_{ao}}\right)x_5$$

$$x_1 = 0.673191, \quad x_2 = 0.479513, \quad x_3 = 1.33335,$$
$$x_4 = 0.882645, \quad x_3 = 0.697106$$

Calculated values versus electrode spacing of this method are shown in Fig. 2*a* by using the same parameters as actual measurements that are reported by Charlton [21].

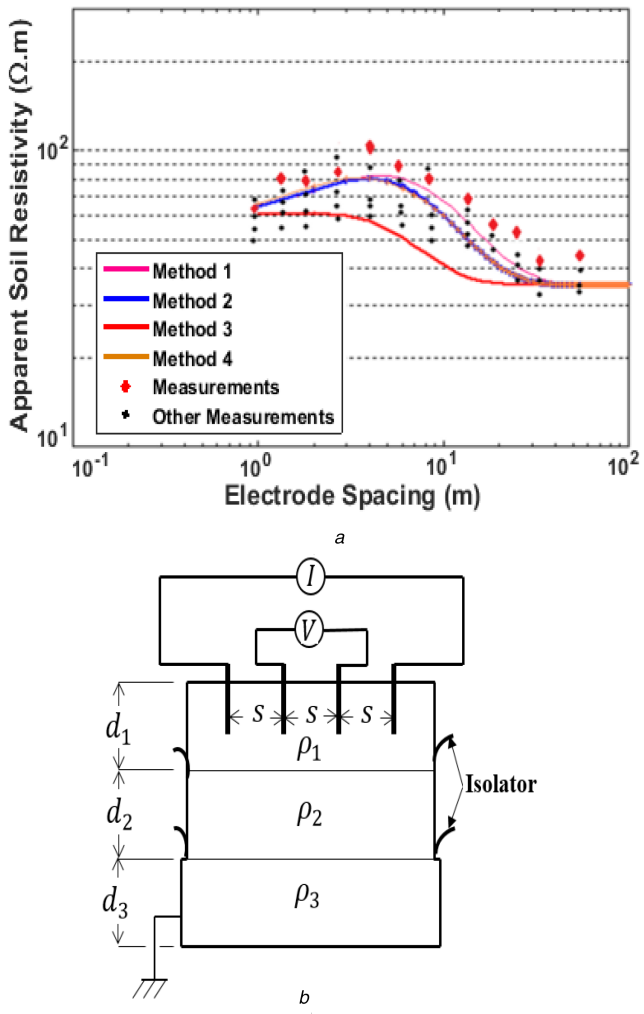

Fig. 2 *Results and experimental setup*
(a) Actual and calculated soil resistivities. Continuous lines represent the calculated soil resistivity and dots simulate the actual site measurements reported by Charlton [21], ***(b)*** Experimental setup

2.4 Fourth method for apparent soil resistivity evaluation

The apparent soil resistivity of the three layers is evaluated by obtaining the initial apparent soil resistivity between the second and the third layers as one layer that its apparent soil resistivity is represented by (ρ_{ao}) using Seedher and Arora equations [28]. Then, the first layer soil resistivity (ρ_1) is taken as second one. Thus, the apparent soil resistivity of the three layers will be as follows **w**hen $(\rho_{ao}) > (\rho_3)$:

$$\rho_a = \rho_1 + 4\rho_1 K_{1a0} \cdot s \cdot \left[\frac{1}{\sqrt{s^2 + 4(d_1)^2}} - \frac{1}{\sqrt{4s^2 + 4(d_1)^2}}\right] + 4\pi V_b \cdot s \cdot \left[\sqrt{\frac{c}{c + (s/(d_1))^\beta}} - \sqrt{\frac{c}{c + (2s/(d_1))^\beta}}\right] \tag{7}$$

where

$$K_{1a0} = \frac{(\rho_{a0} - \rho_1)}{(\rho_{a0} + \rho_1)}$$

$$V_b = \frac{\rho_{a0}(-K_{1a0} - \ln(1 - K_{1a0}))}{2\pi(d_1)}$$

$$\beta = 2 - x_2 \cdot \left[\ln\left(\frac{\rho_3}{\rho_{a0}}\right)\right]$$

$$c = x_1 \cdot \left[\ln\left(\frac{\rho_{ao}}{\rho_1}\right)\right]x_3$$

$$x_1 = 16.4133, \quad x_2 = 0.136074, \quad x_3 = 0.393468$$

However, when $(\rho_{ao}) < (\rho_1)$ the finite expression for apparent resistivity is obtained as follows:

$$\rho_a = \rho_{a0} + \left((\rho_1 - \rho_{a0}) \cdot (2e^{-u_s s} - e^{-u_2 \cdot 2s})\right) \tag{8}$$

where

$$u = u_m - \frac{(u_m - x_1) \cdot e^{-x_2}(s/d_1)}{d_1}$$

$$u_m = x_3 x_4 \left(\frac{\rho_{ao}}{\rho_1}\right)x_5$$

$$x_1 = 0.673191, \quad x_2 = 0.479513, \quad x_3 = 1.33335,$$
$$x_4 = 0.882645, \quad x_3 = 0.697106$$

Calculated values versus electrode spacing of this method are shown in Fig. 2*a* using the same parameters as actual measurements that are reported by Charlton [21].

From this figure, it is found that the measured and calculated results are much closer to each other. More than three soil layers' apparent resistivity can be obtained by using the same techniques. The combination of two layers of the soil together led to neglecting the effect of the current reflection between these two layers, which leads to an increase in the value of the apparent soil resistivity comparing with the field measurements as given in Fig. 2*a*. This increase varies by combining the first layer with the second or merging the second and third layers, as well as using Sunde equations [18] or Seedher and Arora [29] equations in the model calculations.

3 Verification of calculated results

3.1 Experimental setup

The experimental model used to simulate the multilayer soils structure contains three tanks; each one has 1.5 m × 1.5 m and the height of the water in the first one was 0.275 m, the height of the second tank which is completely filled with water was 1.15 m and

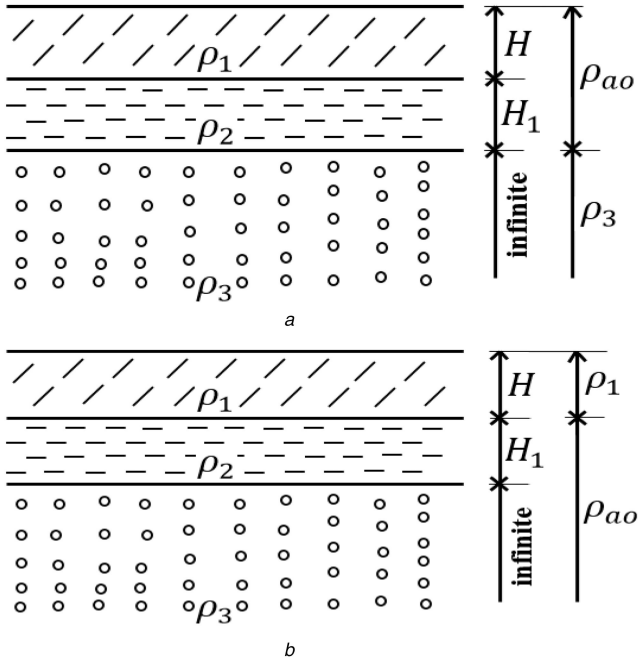

Fig. 3 *Three layers soil model according to IEEE*
(a) First and second layers are evaluated as ρ_{ao}, ***(b)*** Second and third are evaluated as ρ_{ao}

the third tank has 0.5 m and it is also completely filled with water. One tank is installed above the other, the top ends of the lower and the middle tanks are coated with plastic to obtain electrical isolation between the metallic bodies of the three tanks. Only the electrical contact between every two mediums (representing the three layers soil) occurs through the metallic base of the upper tank. The resistivities of the water in the three tanks are controlled by sodium chloride (NaCl) salt to be $\rho_1 = 59\ \Omega$ m, $\rho_2 = 104\ \Omega$ m and $\rho_3 = 35\ \Omega$ m. The water resistivity of each water tank is measured by means of a DC probe. The lower tank is connected to Earth. Wenner method of four electrodes is employed as shown in Fig. 2*b* for the resistivity of multilayer soils simulation measurements. Four copper electrodes with 0.15 m length are used. A 220 V alternating source provided with variac is used to inject the voltage between the voltage electrodes and the current is measured between the two current electrodes. To verify the obtained measurements, the earth tester is used for measuring the three layers' apparent resistivity according to Wenner method. The results are very close to that obtained by voltmeter ammeter method.

3.2 Experimental results

The electric system resistivity is measured using the four electrodes method with changing the space between the electrodes (S). The scale factor for the electrode spacing is considered 1 cm for every 2 m. The measured resistivity is multiplied by the scaling factor of spacing and simulated layers thickness. The obtained results are compared with the calculated values by the four methods and the actual site measurements reported by Charlton [21]. The results are given in Fig. 2*a*. From these results, it is noted that the measured values are slightly different compared with the calculated values, the reason may be due to the boundary effects of the tank walls [30]. Another factor affecting the measurement results is the slight variation in the ionisability of NaCl used to control the water resistivity in the water tanks. The change in solubility and ionisability is over several times of water tanks than weaker electrolytes contained in natural soil used in the field tests that are done by Charlton [21]. This experimental model and its experimental results are not carried out before [31]. The difference between the calculated values of the apparent soil resistivity using the first three methods and the average measured values in the field is between 6 and 0.8% depending on the electrode spacing. This difference increases to 12% compared with the measurements done by using the suggested experimental model.

4 Apparent soil resistivity of multilayer soils according to IEEE

According to IEEE [3], the apparent soil resistivity seen by the ground rods ρ_a is defined as follows:

$$\boldsymbol{\rho}_a = \boldsymbol{l}_2(\boldsymbol{\rho}_1\boldsymbol{\rho}_2)(\boldsymbol{\rho}_2\boldsymbol{H} + \boldsymbol{\rho}_1(\boldsymbol{l}_2 - \boldsymbol{H})) \tag{9}$$

For the case of the rods driven in the same depth as the grid, the apparent soil resistivity can be calculated as follows:

$$\boldsymbol{\rho}_a = \frac{\boldsymbol{l}_2(\boldsymbol{\rho}_1\boldsymbol{\rho}_2)}{(\boldsymbol{\rho}_2(\boldsymbol{H} - \boldsymbol{h}) + \boldsymbol{\rho}_1(\boldsymbol{l}_2 + \boldsymbol{h} - \boldsymbol{H}))} \tag{10}$$

where ρ_1 is the first layer soil resistivity; ρ_2 is the second layer soil resistivity H is the first layer soil thickness h is the laying depth; and l_2 is the length of ground rods.

In this section of this paper, the study is done on three layers that are reduced to one equivalent layer as follows.

4.1 First method

Calculations of initial apparent soil resistivity between first and second layers are done using (10) according to IEEE 80 [3] and it is represented by ρ_{12}, where ρ_1 and ρ_2 are the resistivities of first and second layers, respectively, and H is the thickness of the first layer as shown in Fig. 3*a*. Then to obtain the total apparent soil resistivity of the three layers, the first and the second layers having soil resistivity ρ_{12} are considered as one layer and the third layer resistivities having resistivity ρ_3 are taken as another layer, the apparent soil resistivity is estimated by the following IEEE 80 equation:

$$\rho_a = \frac{l_2(\rho_{12}\,\rho_3)}{(\rho_3(H' - h) + \rho_{12}(l_2 + h - H'))} \tag{11}$$

where ρ_{12} is the apparent soil resistivity between the first and second layers; ρ_3 is the third layer soil resistivity; H' is the thickness of first and second layers; h is the laying depth; and l_2 is the length of ground rods.

The reflection factor is defined in this case as

$$K' = \frac{(\rho_3 - \rho_{12})}{(\rho_3 + \rho_{12})} \tag{12}$$

where ρ_{12} is the apparent soil resistivity between the first and second layer; ρ_3 is the third layer soil resistivity.

4.2 Second method

Calculations are done according to (13) [3] using initial apparent soil resistivity of the third and second layers that is represented by ρ_{23}, where ρ_3 and ρ_2 are the resistivities of third and second layers, respectively; H_1 is the thickness of the second layer; and H is the thickness of the first layer as shown in Fig. 3*b*

$$\boldsymbol{\rho}_{23} = \frac{\boldsymbol{l}_2(\boldsymbol{\rho}_2\boldsymbol{\rho}_3)}{(\boldsymbol{\rho}_3(\boldsymbol{H}_1 - \boldsymbol{h}) + \boldsymbol{\rho}_2(\boldsymbol{l}_2 + \boldsymbol{h} - \boldsymbol{H}_1))} \tag{13}$$

where ρ_{23} is the apparent soil resistivity between the second and third layers; ρ_3 is the third layer soil resistivity; ρ is the second layer soil resistivity; H_1 is the thickness of the second layer; h is the laying depth; and l_2 is the length of ground rods.

Then to obtain the total apparent soil resistivity of the three layers, ρ_{23} is considered as the resistivity of one layer and first soil layer having resistivity ρ_1 is taken as the second layer, the equivalent soil resistivity is calculated by [3]

$$\rho_a = \frac{l_2(\rho_1 \rho_{23})}{(\rho_{23}(H-h)+\rho_1(l_2+h-H))} \quad (14)$$

The reflection factor is defined in this case as

$$K'' = \frac{(\rho_{23} - \rho_1)}{(\rho_{23} + \rho_1)} \quad (15)$$

where ρ_{23} is the apparent soil resistivity of the second and third layers and ρ_1 is the first layer of soil resistivity.

5 Effect of reflection factor on the grid system

5.1 Effect of reflection factor on the apparent soil resistivity

To study the behaviour of grounding grid with reflection factor variation, two multilayer models are used as given in Table 1. One of these parameters is the apparent soil resistivity. Table 2 gives the data used to investigate the factors affecting apparent soil resistivity.

First to explain the effect of the reflection factor on the apparent soil resistivity in three multilayer soils, model (A) soil layers and data given in Table 2 are used. The methods explained in item 4 for calculating the apparent soil resistivity has been employed. The second layer ρ_2 is changed from 20 to 2000 Ω m and the thicknesses of the first layer and also the second layer, each one is taken as 2 m. Fig. 4*a* shows that increasing of the reflection factor decreases the apparent soil resistivity when ($\rho_{12} > \rho_3$). In this case, the reflection factor is positive. This is noted also in the case of ($\rho_3 > \rho_{12}$) when the reflection factor is negative. It is shown in the same figure that in case of ($\rho_1 > \rho_{23}$ or $\rho_3 > \rho_{12}$), the apparent soil resistivity increases with the reflection factor increase.

Similar calculations are done using model (B) data, as shown in both cases ($\rho_{12} > \rho_3$) and ($\rho_3 > \rho_{12}$) the apparent soil resistivity increases with the reflection factor increase. The same when ($\rho_1 > \rho_{23}$ or when $\rho_3 > \rho_{12}$) as given in Fig. 4*b*.

5.2 Effect of reflection factor on the mesh and step voltages

To study the effect of reflection factor on the mesh and step voltages, models (A) and (B) and grounding grid data given in Tables 1 and 2 are used. Mesh and step voltages are calculated according to IEEE 80 equations [3] as follows:

$$\mathbf{Em} = \frac{(i_G\, k_m\, k_3\, \rho_a)}{(l_1 + 1.55\, l_r)} \quad (16)$$

$$\mathbf{Es} = \frac{(i_G\, k_s\, k_3\, \rho_a)}{(l_1 + 0.85\, l_r)} \quad (17)$$

$$k_m = \frac{1}{2\pi}\left[\ln\left(\frac{D^2}{16hd} + \frac{(D+2h)^2}{8Dd} - \frac{h}{4d}\right) + \frac{K_{ii}}{K_h}\ln\frac{8}{\pi(2n-1)}\right]$$

$$\mathbf{Ks} = \frac{1}{\pi}\left[\frac{1}{2h} + \frac{1}{D+h} + \frac{1}{D}(1-0.5^{n-2})\right]$$

where i_G is the maximum grid current that flows between grounding grid and surrounding Earth during faulty condition; k_m is the geometrical factor; K_i is the corrective factor; $\boldsymbol{K}_h$ is the corrective weighting factor that emphasises the effects of grid depth; $\boldsymbol{K}_{ii}$ is the corrective weighting factor that adjusts for the effects of inner conductors on the corner mesh; h is the depth of grounding grid conductors in m; D is the spacing between parallel conductors in metres; d is the diameter of the grid conductor in metres; K_3 is the correction factor for grid geometry; ρ_a is the apparent soil resistivity; $\boldsymbol{l}_1$ is the total length of the grid conductors in metres; and l_r is the total length of grounding rods [3].

Fig. 5*a* shows the step voltage versus the reflection factor using the data of three layers soil model (A) and the data are given in Table 2 of the grounding grid. The step voltage as shown in this figure decreases with the reflection factor increase in both cases ($\rho_{12} > \rho_3$) or ($\rho_3 > \rho_{12}$). However, when ($\rho_1 > \rho_{23}$) or when ($\rho_{23} > \rho_1$) as given in the same figure the step voltage increases with the increase of reflection factor. Similar calculations are done to obtain

Table 1 Values of two models of multilayer soils

Model	Layer	Resistivity, Ω m	Thickness, m
A	1	200	2
	2	20–2000	2
	3	300	∞
B	1	200	2
	2	1000	2
	3	20–2000	∞

Table 2 Data used to investigate the factors affecting apparent soil resistivity

area	100 × 100 m^2
surface resistivity	3000 Ω m
thickness of surface-crashed rock	0.2 m
thickness of the upper layer	2 m
fault current	6000 A
number of rods	20
length of rods	6 m
space between each two conductors	3 m
laying depth	0.5 m

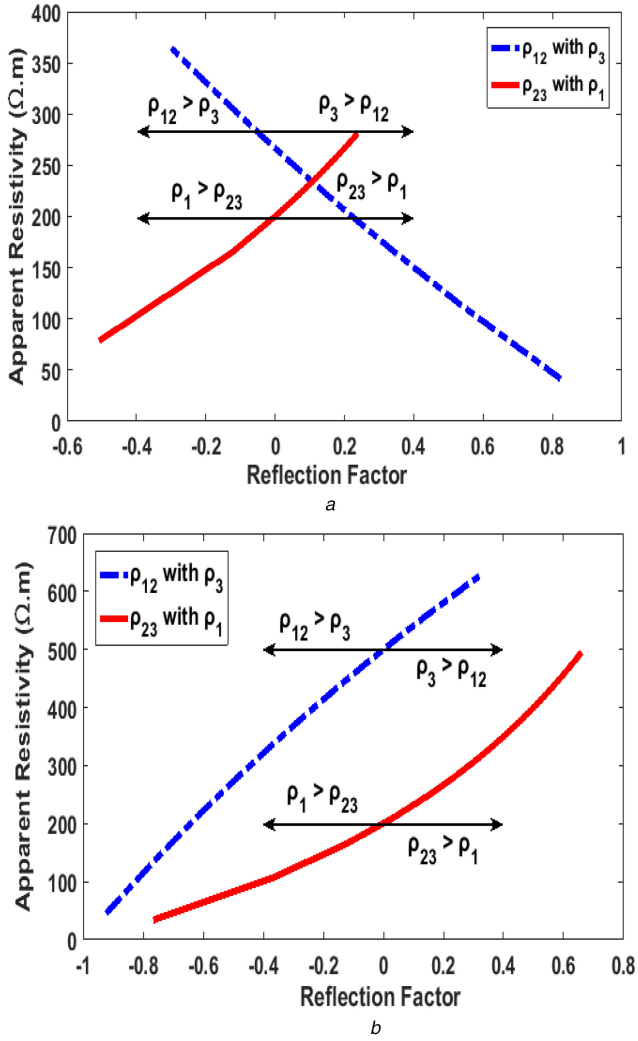

Fig. 4 *Relation between the reflection factor and apparent soil resistivity*
(a) Using the data of multilayers soil models (A) given in Tables 1 and 2, ***(b)*** Using the data of three-layer soil model (B) given in Tables 1 and 2

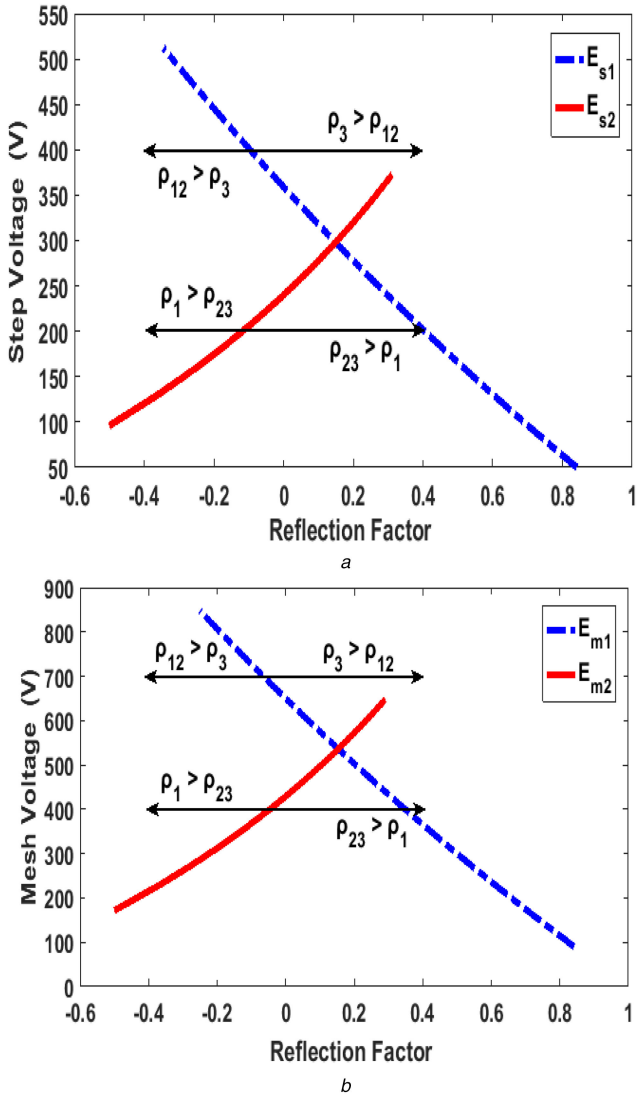

Fig. 5 *Relation between the reflection factor and step voltage*
(a) Using the data of three layers soil model (A) and the grounding grid specifications given in Tables 1 and 2, ***(b)*** Using the data of three-layer soil model (B) and the grounding grid specifications given in Tables 1 and 2

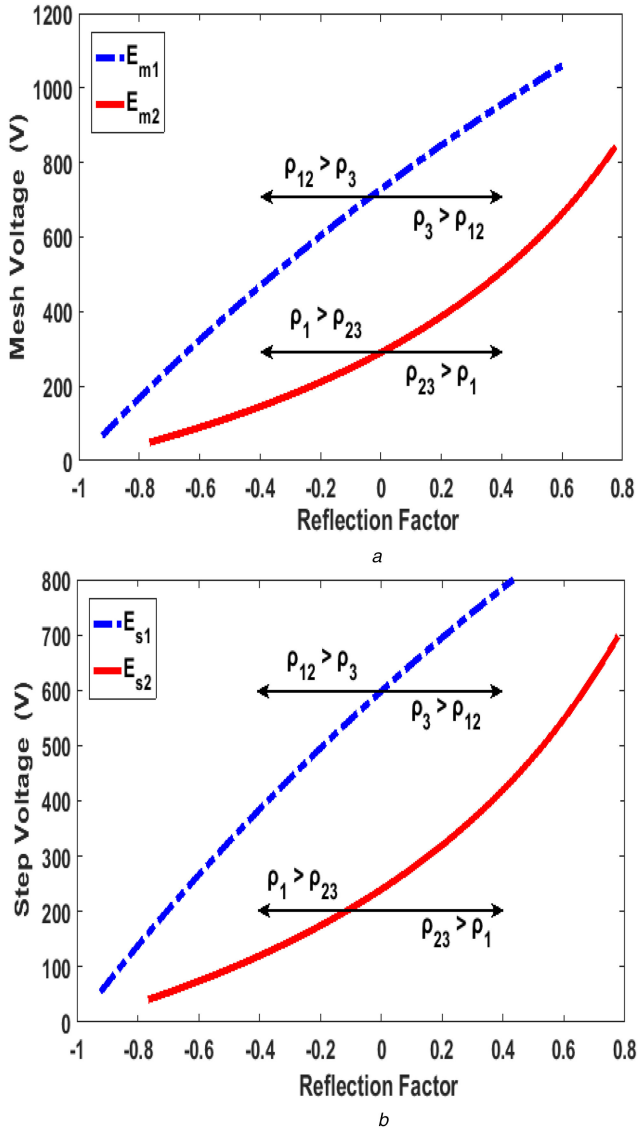

Fig. 6 *Relation between the reflection factor and the mesh voltage*
(a) Using the data of three layers soil model (A) and the grounding grid specifications given in Tables 1 and 2, ***(b)*** Using the data of multilayers soil models (B) and the grounding grid specifications given in Tables 1 and 2

the relation between the reflection factor and mesh voltage as given in Fig. 5*b*. As it is noted in this figure, the relation between the mesh voltage and the reflection factor has a similar characteristic of the step voltage versus the reflection factor.

Similar calculations are done to calculate the step and touch voltages using three layers soil model (B) data and the data of the grounding grid given in Table 2, as shown in Figs. 6*a* and *b* the mesh and step volts increase with the reflection factor increase in cases of ($\rho_{12} > \rho_3$), ($\rho_3 > \rho_{12}$), ($\rho_1 > \rho_{23}$) and when ($\rho_{23} > \rho_1$).

The voltage profiles of the grid under study in different cases in three dimensions are given in Fig. 7. The description of each case given in Fig. 7 is tabulated in Table 3.

As it is noted in Figs. 7*a* and *b*, the voltage profiles when taking the first and the second layers as one layer and the third layer as another layer have the same profile when the second and the third layers are considered as one layer and the first layer is taken as another. The difference is that the case (a) profile voltage values are higher than that obtained in case (b). The same is noted with increasing the number of conductors as given in Figs. 7*c* and *d*. It is noted also that increasing the conductor's number gives a smoother voltage profile.

5.3 Effect of the reflection factor on the ground grid resistance

To study the effect of reflection factor on the grounding grid resistance, the data of the three layers soil models (A) and (B) and also the grounding grid specifications given in Tables 1 and 2 are employed. The calculations are done by using IEEE 80 equations [3]

$$R1 = (\rho_1/\pi\, l_1)(\ln(2l_1/h\,) + k_1(l_1/\sqrt{A}) - K_2) \tag{18}$$

$$R2 = (\rho_a/2n\pi\, l_2)(\ln(8l_2/d_2) - 1 + 2k_1(l_1/\sqrt{A})(\sqrt{n} - 1)^2) \tag{19}$$

$$R12 = (\rho_a/\pi\, l_1)(\ln(2l_1/l_2) + k_1(l_1/\sqrt{A}) - K_2 + 1) \tag{20}$$

$$Rg = \frac{R_1R_2 - R_{12}^2}{R_1 + R_2 - 2R_{12}} \tag{21}$$

where Rg is the grounding system resistance; R_1 is the resistance of grid conductors; R_2 is the resistance of the ground rods; R_{12} is the mutual resistance between the grid conductors and grounding rods; ρ_1 is the soil resistivity encountered by grid conductors buried at depth h in Ω m; ρ_a is the apparent soil resistivity as seen by a ground rod in Ω m; H is the thickness of the upper layer soil in m; ρ_2 is the soil resistivity from depth H downward in Ω m; l_1 is the total length of grid conductors in m; l_2 is the average length of a ground rod in m; h is the depth of grid burial in m; h' is defined as $\sqrt{d_1h}$ according to IEEE 80 [3]; A is the area covered by a grid of

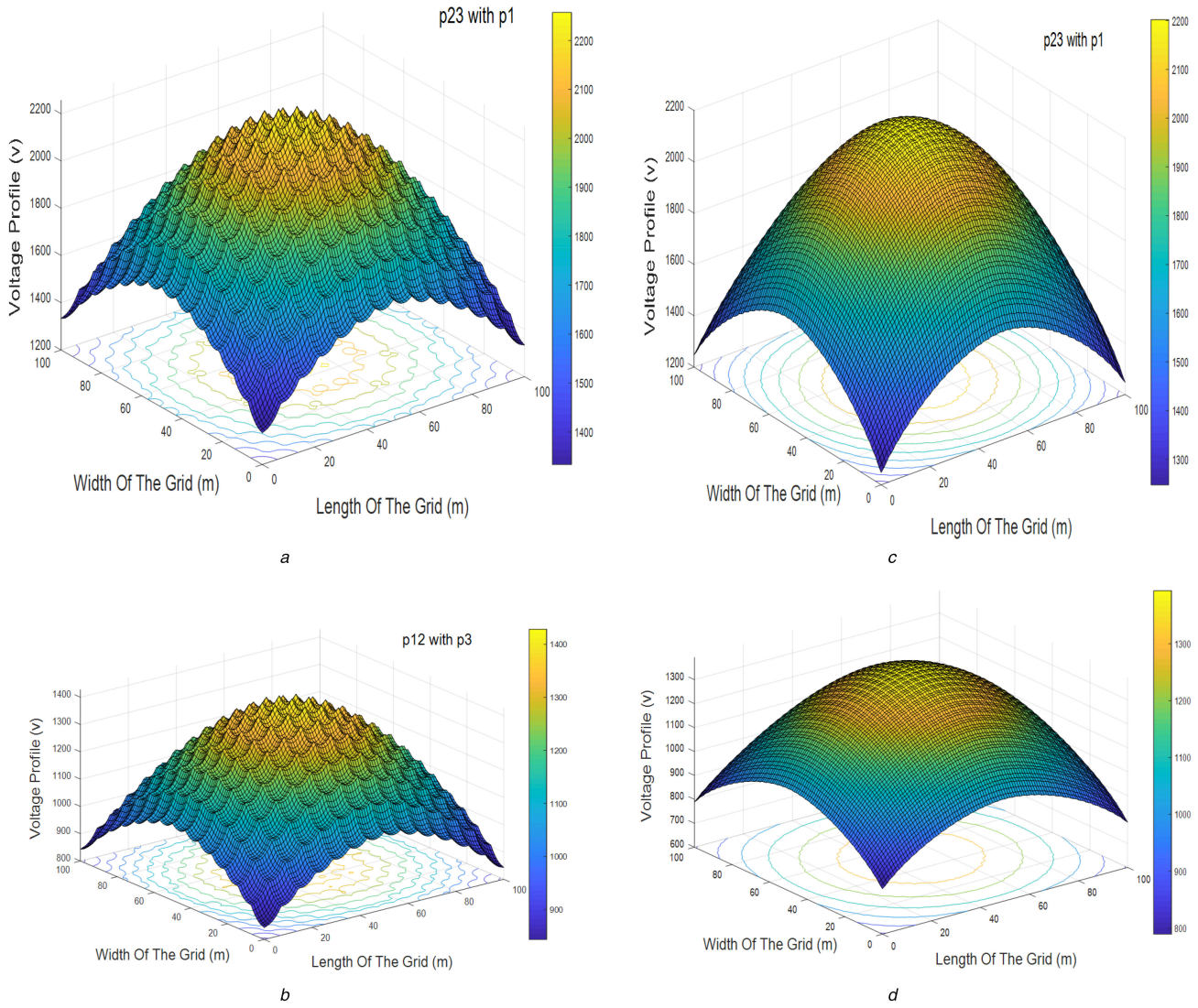

Fig. 7 *Voltage profiles of the grid under study in different cases in three dimensions* ***(a)***, ***(b)***, ***(c)***, ***(d)*** as given in Table 3

Table 3 Cases description of Fig. 7

Case	Description
(a)	$\rho_1 = 200\ \Omega$ m, $\rho_2 = 50\ \Omega$ m and $\rho_3 = 300\ \Omega$ m; the thickness of the first layer = 2 m, thickness of the second layer = 2 m, rod length = 6 m, laying depth = 0.5 m, number of conductors = 15, square grid equally spaced and ρ_{12} is taken as one layer with ρ_3 as the second layer
(b)	same data of the grid and layers as (a), but ρ_{23} is taken as one layer with ρ_1 as the second layer
(c)	$\rho_1 = 200\ \Omega$ m, $\rho_2 = 50$ and $\rho_3 = 300\ \Omega$ m, the thickness of the first layer = 2 m, the thickness of the second layer = 2 m, rod length = 6 m, laying depth = 0.5 m, number of conductors = 34, equally spaced and ρ_{12} is taken as one layer with ρ_3 as the second layer
(d)	same data of the grid and layers as (c), but ρ_{23} is taken as one layer with ρ_1 as the second layer

dimensions, m^2; n is the number of ground rods placed in the grid area A; and K_1, K_2 are constants related to the geometry of the system as reported by [3].

Fig. 8*a* shows the effect of reflection factor on the grounding grid resistance using the data of model (A) and the grounding grid specifications given in Tables 1 and 2. It is noted that when $\rho_1 > \rho_{23}$, the ground grid resistance increases until reaching to uniform soil condition ($\rho_1 = \rho_{23}$), the reflection factor, in this case, is zero. After that value increasing the reflection, factor leads to a sharp decrease in grounding grid resistance. Similar results are obtained when $\rho_{12} > \rho_3$ until reaching to reflection factor equals 0.3, then the resistance of the grid increases, but after that the grid resistance decreases. From calculations done by using model (B) data and the grounding grid specifications are given in Tables 1 and 2, it is noted as given in Fig. 8*b* that when $\rho_1 > \rho_{23}$ the grounding grid resistance increases until reflection factor equals –0.3, after that it decreases, but when $\rho_{12} > \rho_3$ the ground grid resistance increases until reaching to $\rho_{12} = \rho_3$, after that it decreases. Fig. 8*c* shows additional relation between the reflection factor and ground resistance when $\rho_1 = 200\ \Omega$ m; ρ_3 is taken 20–2000 Ω m and $\rho_2 = 100\ \Omega$ m, the thickness of the first layer = 2 m, a thickness of the second layer = 2 m and each rod length = 6 m.

6 Supporting of calculated results of reflection factor effects on the grounding grid parameters by experimental measurements

For the verification of the calculated results of the effect of reflection factor on the mesh and step voltages and the grid resistance, the experimental model given in Fig. 2*b* is modified as shown in Fig. 8*d*. The modified model contains only two identical tanks. They are filled with tap water. The lower tank is connected

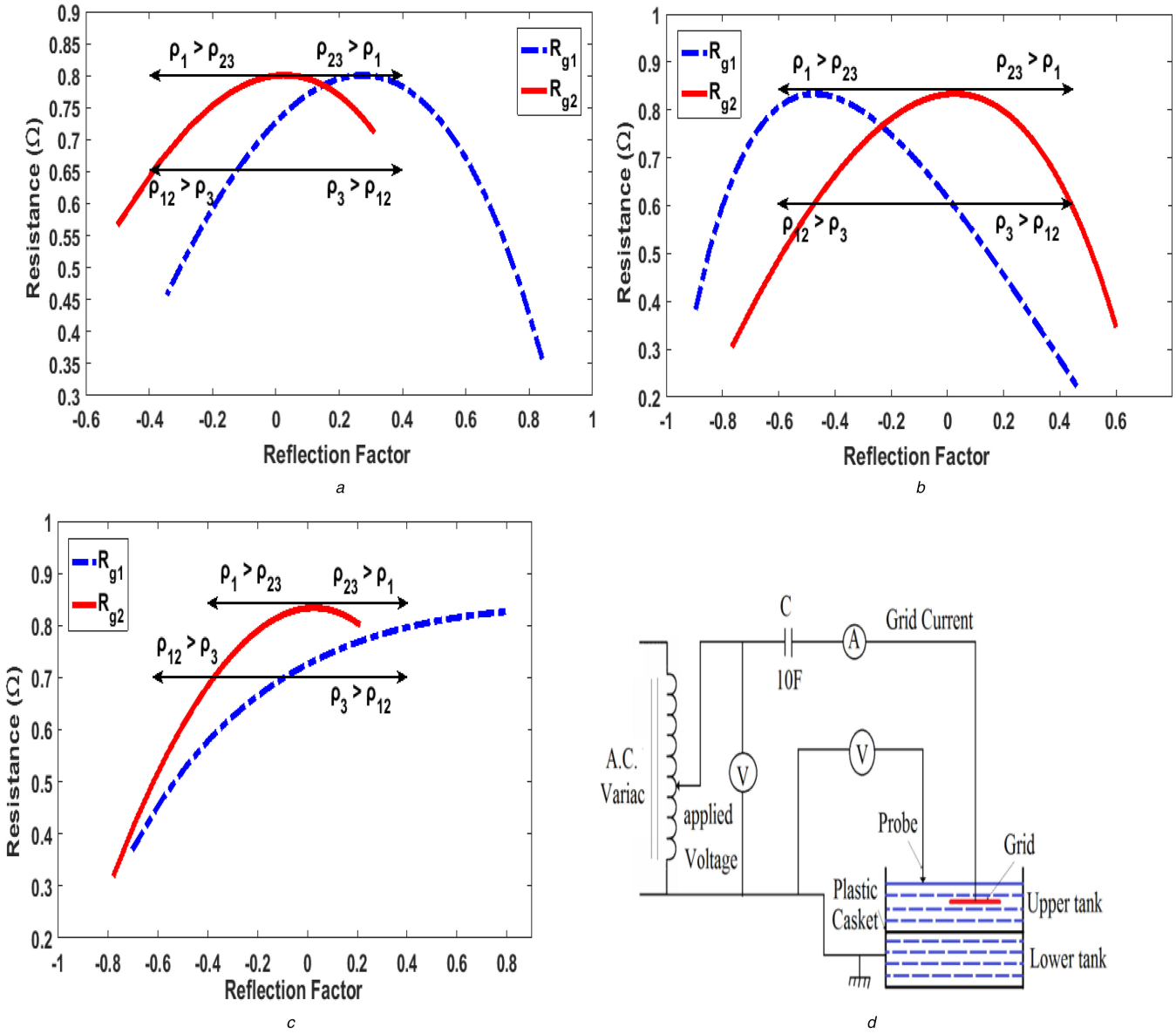

Fig. 8 *Calculated results and the modified experimental setup*

(a) Effect of reflection factor on the grounding grid resistance using the data of model (A) and the grounding grid specifications given in Tables 1 and 2, ***(b)*** Effect of reflection factor on the grounding grid resistance using the data of model (B) and the grounding grid specifications given in Tables 1 and 2, ***(c)*** Additional relation between the reflection factor and ground resistance when $\rho_1 = 200\ \Omega$ m, ρ_3 is taken 20–2000 Ω m and $\rho_2 = 100\ \Omega$ m, thickness of the first layer = 2 m, thickness of the second layer = 2 m and each rod length = 6 m, ***(d)*** Modified experimental setup

to Earth. The resistively of the upper and lower water layers are controlled by adding an amount of NaCl to simulate the two multilayer soils. Each one of the three-layer models (A) and (B) given in Table 1 is reduced to two layers model as explained before. The water resistivities in the upper and lower tanks of the simulated model are controlled to be in agreement with the soil resistivity values used in the calculations given in Figs. 5*a* and *b*, 6*a* and *b* and 8*a* and *b*. The water conductivity is measured by means of a DC probe. A 220 V alternating source provided with variac is connected with the grounding grid model which is suspended in the upper tank.

Capacitor (10 F) is connected between the variac and the grid model to prevent any flow of DC current due to the use of dissimilar materials.

Two voltmeters are used: one for measuring the input voltage to the model and the other is connected to a probe for measuring the voltage distribution on the grid surface. One ammeter is used to measure the input grid current that simulates the short-circuit current, as shown in Fig. 8*d*. The grounding grid $100 \times 100\ \text{m}^2$ data given in Table 2 is simulated with a chosen scale factor of 1/100. In the opinion of several researchers, the effects of grid conductor diameter on grid resistance and the earth surface potentials are negligible [30]. The simulated grid conductors are made from copper having 2.5 mm in diameter. The scale factor of the grid laying depth and the upper layer thickness is chosen to be 1/100. Table 4 gives a summary of calculated and measured values of step and touch voltages and grounding grid resistance as a function of the reflection factor. It is noted that the measured values are slightly higher than that calculated. In the author's opinion, that is, may be due to the boundary effects of the tank walls. Another factor affecting the measurement results is the slight variation in the ionisability of NaCl used to control the water resistivity in the tanks that contain a large amount of water.

7 Conclusion

This paper contains different strategies for calculating the apparent soil resistivity using Sunde, Seedher and Arora equations. Comparisons to the field measurements carried out by others and experimental model measurements done by the authors are done. It is noted that the first three methods are very close to each other and also close to the experimental findings. The fourth method gives some tolerance with the first three when the space between the rods is <15 m, but it is in agreement with the experimental

Table 4 Summary of calculated and measured values

Figs. 5*a* and *b* verification									
reflection factor	−0.8	−0.6	−0.3	−0.2	0	0.2	0.4	0.6	0.8
step voltage, volt, calculated, $\rho_{12} > \rho_3$ or $\rho_3 > \rho_{12}$	—	—	480	440	350	275	200	125	60
step voltage, volt, measured, $\rho_{12} > \rho_3$ or $\rho_3 > \rho_{12}$	—	—	490	460	355	276	210	128	63
step voltage, volt, calculated, $\rho_1 > \rho_{23}$ or when $\rho_{23} > \rho_1$	—	—	100	175	245	330	400	—	—
step voltage, volt, measured, $\rho_1 > \rho_{23}$ or when $\rho_{23} > \rho_1$	—	—	104	180	250	332	410	—	—
mesh voltage, calculated $\rho_{12} > \rho_3$ or $\rho_3 > \rho_{12}$	—	—	820	800	640	500	360	230	105
mesh voltage, volt, measured, $\rho_{12} > \rho_3$ or $\rho_3 > \rho_{12}$	—	—	825	810	645	505	364	232	107
mesh voltage, volt, calculated, $\rho_1 > \rho_{23}$ or when $\rho_{23} > \rho_1$	—	—	260	300	400	580	750	—	—
mesh voltage, volt, measured, $\rho_1 > \rho_{23}$ or when $\rho_{23} > \rho_1$	—	—	266	306	405	582	752	—	—
Figs. 6*a* and *b* verification									
reflection factor	−0.8	−0.6	−0.4	−0.2	0.0	0.2	0.4	0.6	0.8
mesh voltage, volt, calculated, $\rho_{12} > \rho_3$ or $\rho_3 > \rho_{12}$	180	250	420	606	700	805	870	1020	—
mesh voltage, volt, measured, $\rho_{12} > \rho_3$ or $\rho_3 > \rho_{12}$	185	254	427	611	722	809	880	1029	—
mesh voltage, volt, calculated, $\rho_1 > \rho_{23}$ or when $\rho_{23} > \rho_1$	30	85	175	200	280	390	480	610	820
mesh voltage, volt, measured, $\rho_1 > \rho_{23}$ or when $\rho_{23} > \rho_1$	40	90	280	205	284	394	484	615	824
step voltage, calculated $\rho_{12} > \rho_3$ or when $\rho_3 > \rho_{12}$	130	270	395	500	600	700	780	—	—
step voltage, volt, measured, $\rho_{12} > \rho_3$ or when $\rho_3 > \rho_{12}$	140	275	400	520	608	710	790	—	—
step voltage, volt, calculated, $\rho_1 > \rho_{23}$ or when $\rho_{23} > \rho_1$	40	70	105	180	230	305	610	550	—
step voltage, volt, measured, $\rho_1 > \rho_{23}$ or when $\rho_{23} > \rho_1$	43	74	110	184	236	310	617	560	—
Figs. 8*a* and *b* verification									
reflection factor	−0.5	−0.4	−0.3	−0.2	0.0	0.2	0.4	0.6	0.8
grounding resistance, Ω, calculated, $\rho_1 > \rho_{23}$ model A	0.57	0.63	0.72	0.74	0.8	0.77	—	—	—
grounding resistance, Ω, measured, $\rho_1 > \rho_{23}$ model A	0.6	0.68	0.74	0.76	0.82	0.8	—	—	—
grounding resistance, Ω, calculated, $\rho_{12} > \rho_3$ model A	—	—	0.45	0.6	0.73	0.77	0.87	0.67	0.8
grounding resistance, Ω, measured, $\rho_{12} > \rho_3$ model A	—	—	0.5	0.63	0.74	0.79	0.89	0.7	0.86
grounding resistance, Ω, calculated, $\rho_1 > \rho_{23}$ model B	—	0.68	—	0.78	0.84	0.8	0.62	0.35	—
grounding resistance, Ω, measured, $\rho_1 > \rho_{23}$ model B	—	0.73	—	0.8	0.86	0.83	0.65	0.4	—
grounding resistance, Ω, calculated, $\rho_{12} > \rho_3$ model B	—	0.82	—	0.75	0.6	0.45	0.25	—	—
grounding resistance, Ω, measured, $\rho_{12} > \rho_3$ model B	—	0.85	—	0.78	0.66	0.5	0.3	—	—

measurements. The differences in the measured values in the field on one side and that obtained by using a laboratory model on the other side may be due to the boundary effects of the used model. Another factor affecting the measurement results is the variation in the ionisability of NaCl used to control the water resistivity. The change in solubility and ionisability of water tanks is over several times than weaker electrolytes contained in natural soil used in the field tests that are done by the others.

It is concluded also that the reflection factors in non-uniform soil have significant effects on the apparent soil, step and mesh voltages and ground resistance of the grid. For the verification of the calculated results, experimental model is used. It is noted that the measured values are slightly high compared with the calculated values; the reason as mentioned above may be due to the boundary effects of the used model.

8 References

[1] Dwight, H.B.: 'Calculation of resistance to ground', *Electr. Eng.*, 1936, **55**, p. 1319

[2] Nahman, J., Skuletich, S.: 'Resistance to ground and mesh voltage of ground grid', *Proc. IEE*, 1979, **126**, (1), pp. 57–61

[3] IEEE 80-2000: 'Guide for safety in AC substation grounding', IEEE, 2000

[4] Gouda, O.E., Amer, G.M., EL-Saied, T.M.: 'Optimum design of grounding system in uniform and non-uniform soils using ANN', *Int. J. Soft Comput.*, 2006, **1**, (3), pp. 175–180

[5] Sverak, J.G.: 'Simplified analysis of electrical gradients above a ground grid', *IEEE Trans. Power Appar. Syst.*, 1984, **PAS-103**, (1), pp. 7–25

[6] Schwarz, S.J.: 'Analytical expressions for the resistance of grounding systems', *AIEE Trans. Power Appar. Syst.*, 1954, **73**, Part III-B, pp. 1011–1016

[7] Nahman, J.M., Salamon, D.D.: 'Analytical expressions for the resistance of grounding grids in non-uniform soil', *IEEE Trans. Power Appar. Syst.*, 1984, **PAS-103**, pp. 880–885

[8] Sullivan, J.A.: 'Alternative earthing calculations for grids and rods', *IEE Proc. Transm. Distrib.*, 1998, **145**, (3), pp. 271–280

[9] Zaini, H.G., Ghoneim, S.S.: 'Earth surface potential and grounding resistance for grounding grid in two-layer model soil'. 2012 IEEE Int. Conf. Power System Technology (POWERCON), Hebei, China, 2012

[10] Chow, Y.L., Salama, M.M.A.: 'A simplified method for calculating the substation grounding grid resistance', *IEEE Trans. Power Deliv.*, 1994, **9**, (2), pp. 736–742

[11] Dawalibi, F., Mukhedkar, D.: 'Optimum design of substation grounding in a two layer earth structure: part I – analytical study', *IEEE Trans. Power Appar. Syst.*, 1975, **PAS-94**, (2), pp. 252–261

[12] He, J., Zeng, R., Gao, Y., *et al.*: 'Optimal design of grounding system considering the influence of seasonal frozen soil layer', *IEEE Trans. Power Deliv.*, 2005, **20**, (1), pp. 107–115

[13] Sun, W., Jingling, H., Yanqing, G., *et al.*: 'Optimal design analysis of grounding grids for substations built in non-uniform soil', IEEE Int. Conf. on Power System Technology, Perth, Australia, 2000, pp. 1455–1460

[14] Thabet, A.: 'Grounding systems of electric substations in non-uniform earth structure with new analysis'. MSc thesis, High Institute of Energy, Aswan, 2002

[15] Phithakwong, B., Kraisnachinda, N., Banjongjit, S., *et al.*: 'New techniques the computer-aided design for substation grounding'. IEEE Power Engineering Society Winter Meeting, Singapore, 2000, vol. **3**, pp. 2011–2015

[16] Gouda, O.E., El Dein, A.Z.: 'Ground potential rise of faulty substations having equal and unequal spacing grounding grids conductors', *IET Gener. Transm. Distrib.*, 2017, **11**, (1), pp. 18–26

[17] Gouda, O.E., Amer, G.M., Ibrahim, H.: 'Surface potentials and GPR of substation grounding'. Cired, 21st Int. Conf. Electricity Distribution, Frankfurt, 6–9 June 2011, p. 20

[18] Sunde, E.D.: '*Earth conduction effects in transmission systems*' (Dover Publications, New York, USA., 1968)

[19] Schon, J.H.: 'Physical properties of rocks: fundamentals and principles of petro-physics', '*Handbook of geophysical exploration*', vol. **18** (Pergamon, USA., 1998)

[20] Takahashi, T., Kawase, T.: 'Calculation of earth resistance for a deep driven rod in a multi-layer earth structure', *IEEE Trans. Power Deliv.*, 1991, **PWRD-6**, (2), pp. 608–614

[21] Charlton, T.: 'Substation earthing-shedding light on the black art'. IEE Seminar, Birmingham, March 2000

[22] Takahashi, T., Kawase, T.: 'Analysis of apparent resistivity in a multi-layer earth structure', *IEEE Trans. Power Deliv.*, 1991, **5**, (2), pp. 604–610

[23] Del Alamo, J.L.: 'A comparison among eight different techniques to achieve an optimum estimation of electrical grounding parameters in two-layered earth', *IEEE Trans. Power Deliv.*, 1993, **8**, (4), pp. 1890–1899
[24] Lagacé, P.J., Fortin, J., Crainic, E.D.: 'Interpretation of resistivity sounding measurements in *N*-layer soil using electrostatic images', *IEEE Trans. Power Deliv.*, 1996, **11**, (3), pp. 1170–1349
[25] Slaoui, F.H., Georges, S., Lagacé, P.J., *et al.*: 'The inverse problem of Schlumberger resistivity sounding measurements by ridge regression', *Electr. Power Syst. Res. J.*, 2003, **67**, (2), pp. 109–114
[26] Slaoui, F., Georges, S., Lagacé, P.J., *et al.*: 'Fast processing of resistivity sounding measurements in *N*-layer soil'. Proc. IEEE Power Engineering Society 2001 Summer Meeting, Vancouver, Canada, 2001
[27] Lagace, P.J., Vuong, M.N.: 'Graphical user interface for interpreting and validating soil resistivity measurements'. Proceeding of the IEEE ISIE 2006, Montreal, Canada, 2006, pp. 1841–1845
[28] Salama, S., Sattar, S.A., Shoush, K.O.: 'Comparing charge and current simulation method with boundary element method for grounding system calculations in case of multi-layer soil', *Int. J. Electr. Comput. Sci.*, 2012, **12**, (4), pp. 17–24
[29] Seedher, H.R., Arora, J.K.: 'Estimation of two layer soil parameters using finite Wenner resistivity expressions', *IEEE Trans. Power Deliv.*, 1992, **PWDR 7**, (3), pp. 1213–1217
[30] Gouda, O.E.: '*Design parameters of electrical network grounding systems*' (ICI Global Publications, USA., 2017)
[31] Gouda, O.E., Amer, G.M., EL-Saied, T.M.: 'Factors affecting the apparent soil resistivity of multi-layer soil'. Proc. XIVth Int. Symp. High Voltage Engineering, Tsinghua University, Beijing, China, 25–29 August 2005